Manipulation of Mass Transport Rates using Bead-in-a-tube Method

Nicolas E. F. Uhnak[1], Samuel S. Morrison[1], Matthew J. O'Hara[1], Nathaniel J. Murray[1], Michael S. Bartsch[2], Harrison S. Edwards[2], and Jay W. Grate[1]

[1]Pacific Northwest National Laboratory: 902 Battelle Blvd., P.O. Box 999, Richland, WA 99354, USA.

[2]Sandia National Laboratory: Sandia National Laboratories, California, P.O. Box 969, Livermore, CA 94550, USA

Corresponding author: Nicolas.uhnak@PNNL.gov

Keywords: Plutonium, Anion Exchange, Rate constants, Single Bead, Bead-in-a-tube

Abstract

In ultralow Pu analyses, the gold standard is thermal ionization mass spectrometry (TIMS), which requires pure sources to achieve its performance. This purity is achieved through step-wise purifications. In this work single, anion-exchange beads were trapped in the tubing to allow for dynamic solution cycling over the surface of the beads to improve the rates of metal complex uptake. Rates of Pu sorption on single ~900 μm SIR-1200 and ~620 μm Reillex-HPQ beads were determined for single beads trapped in a tube with syringe pump driven dynamic solution cycling over the bead, improving sorption and desorption rates. A static control was used as a comparison. Using ^{238}Pu to enable facile activity-based measurements, rates were determined by measuring the residual Pu after contact with beads using liquid scintillation analysis (LSA) for fixed periods of time. Syringe pump driven dynamic solution cycling results in ~5 and ~15-fold improvements in the sorption rates for SIR-1200 and Reillex-HPQ. Impacts on desorption were also examined.

Introduction

In ultralow Pu analyses, whether for forensics, safeguards, or fallout measurements, the signatures are typically in quantities that preclude the use of standard radio-analytical techniques, thus requiring techniques that possess excellent isotopic composition information, exceptional isotopic resolution with high precision and an extremely low detection limit like those found with TIMS (Thermal Ionization Mass Spectrometry) [1-4]. A number of step-wise analyte isolation and volume reductions steps are taken to obtain a sufficiently pure TIMS analyte source; this process requires an effective means for small volume micro-chemical purification processing [1,5-8].

Many of the steps utilize anion exchange as the primary means of isolating and concentrating the Pu. This separation utilizes the capability of the actinides (oxidation states 4-6) to form anionic nitrate complexes such as $Pu(NO_3)_6^{2-}$. More than 50 years has been devoted to the purification and study of Pu using anion exchange processes [9-14]. Ion-exchange is mass-transport-controlled [8,15]. The $Pu(NO_3)_6^{2-}$ ions have slow rates of mass transport (requiring times up to three weeks to reach equilibrium), which can be overcome by using more resin, but this is not an option for the TIMS sample preparation [1,5,7-14,20]. Mass transport mechanism dictates the rates at which the Pu complexes can sorb or desorb from the anion exchange media, but for the sake of this work, film diffusion is the primary transport mechanism [12-16]. Film diffusion is the movement of the bulk analyte through a depletion zone to the surface of the bead [12,15,16]. Rates of sorption and desorption vary with functional groups on the bead [9,12-14,17]. Pu desorption rates are faster from pyridinium groups relative to tetraalkylammonium groups [12-14,17]. Advanced resin materials exist, but are largely outside of the scope of this work [17-21].

Methods to improve rates have been investigated [7,8,15,18]. It has been noted that agitation of the solution results in a significant improvement in the sorption rates on singles beads [7]. In one such investigation, Pu separation on a single anion exchange bead was examined using acoustic streaming to improve sorption rates [8]. Acoustic streaming uses ultrasonic sound to induce convection in the solution, causing diffusion layer thinning and improving rates [8,15]. Rates were found to increase up to ~9 times relative to stationary controls.

In this work the bead-in-a-tube method was investigated as a method to improve the state of practice, the apparatus is shown in figure 1. The bead-in-a-tube method allows for solution manipulation by a syringe pump, while maintaining an environment that reduces the possibility of contaimination while conducting micro-chemical purifications. The solution was cycled through this apparatus, providing convection, altering the mass transport rates. Sorption and desorption rates were examined under dynamic and static conditions, measuring ^{238}Pu activity after contact with the bead for lengths of time. To the author's knowledge this work represents the second report of the rate constants of Pu sorption (reference 8), and the first report of desorption rate constants on single anion exchange beads.

Figure 1 here

Theoretical

Rate Calculations

The capacity of the SIR-1200 beads is 1.4 meq/cm^3 (value provided by ResinTech). A value for the Reillex-HPQ resin is reported as 182 g/L resin [12]. Using the values above, the capacities of the beads exceed the moles of the sample by a factor of 61 and 41 for the 900 μm and 600 μm SIR-1200 beads respectively, while for the Reillex-HPQ the functional groups exceed the Pu solution concentration by a factor of 10. The relative excess of the functional groups relative to [Pu] allows for the treatment of the rates of sorption and desorption as pseudo first order in the rate analysis [15,16]. The determination of the rate constants analyzed the initial rates rather than the equilibrium conditions and are reported with the uncertainty found in the linear fit from Origin 2017. Equation 1 describes the sorption of the analyte as it is reduced to a fraction of its initial concentration in a constant volume batch operation [8,22].

$$\ln(X) = -k_{obs}t = -\left(\frac{3\overline{V}D}{r_0 V \delta}\right)t \qquad \mathbf{1}$$

where X is the fraction of analyte in solution at time t (s), k_{obs} is the observed rate constant of the exchange reaction, V is the volume of solution, $\overline{V}$ is the volume of the ion exchange media, r_0 is the radius of the ion-exchange bead (on average), D is the diffusion coefficient of the analyte, and δ is the Nernst diffusion radius or diffusion layer thickness.

Two parameters within the rate equation are adjusted under forced convection, those being the diffusion coefficient (eq. 2) and the diffusion layer thickness (D and δ respectively) [9]. Where kT is the thermal energy (J), a is the hydrodynamic radius of the analyte, η is the viscosity of the solution containing the analyte.

$$D = \frac{kT}{6\pi a \eta} \qquad \mathbf{2}$$

Under isothermal conditions, it can be assumed that the diffusion coefficient is nearly constant, leaving only the diffusion layer thickness (δ) to be responsible for altering the rates of mass transport. Diffusion layer thickness calculations for Pu sorption make use of the 1.791x10^{-10} m^2/s diffusion coefficient used in the static conditions found in the work by Paxton et al in conditions similar to those used in this study, though other conditions have been reported [8,24-26]. The average room temperature was 22 ± 2 ^{o}C, therefore isothermal conditions were assumed over the experimental time frame. The diffusion layer thickness is defined in equation 3

$$\delta = \frac{0.2 r_0}{(1 + 70 r_0 v)} = \frac{3\overline{V}D}{r_0 V k_{obs}} \qquad \mathbf{3}$$

where r_0 is the bead radius (cm) and v is the linear flow velocity (cm/s) [6]. Hence, changing the flow rate over the bead surface will change the diffusion layer thickness. Diffusion layer thickness was not determined for desorption, due to the complicated chemistry of Pu during the desorption process [27].

Methods and Materials

SIR-1200 resin was purchased from ResinTech (West Berlin, NJ), selected due to its mechanical strength, similar sorption properties to alternative anion exchange media, and is commercially available in the size range required for this work. The beads were sieved to isolate 850-1000 μm, and 550-700 μm beads using a series of consecutive metal sieves from Retsch GMbH & Co and AS 200 digit cA vibratory sieve shaker, allowing for large quantities of beads to be isolated in a relatively narrow size range. These beads were rehydrated prior to use in 7.5 M HNO_3. Reillex-HPQ beads were purchased from Vertellus (Indianapolis, IN) and stored hydrated in >18 MΩ•cm water. Reillex-HPQ was selected as a candidate for study due to the rapid mass transport properties and high resistance to acidic and radiological degradation found by Marsh et al. and is within the size ranges required for this work [19-21]. A calibrated DinoLite digital microscope was used to isolate 620 (30) μm (value represents the average of isolated >100 beads and 1σ of that value) diameter beads by hand.

All acid reagents (HNO_3 and HCl) were Optima grade received from Fisher Scientific (Pittsburgh, PA), and all solutions used 18.2 MΩ•cm water. The ^{238} Pu was received from an internal Pacific Northwest National Laboratory (PNNL) stock, containing 8900 Bq/mL in 7.5 M HNO_3. Valence was not controlled beyond the use of high HNO_3 or HCl concentrations both of which stabilize the tetravalent oxidation state in solution [27]. Quantification or liquid scintillation counting (LSC) of ^{238}Pu pre- and post-bead contact activity was performed using a Perkin-Elmer Tri-Carb 3100 liquid scintillation analyzer (LSA). The ^{238}Pu activity in the samples was counted for 3 minutes or until the uncertainty (2σ%) in the counted activity reached 1% by LSC. All LSC analyses were conducted using 10 mL of Ultima Gold AB liquid scintillation cocktail.

Static sorption and desorption

Static solution experiments were conducted using polystyrene 384-well microplates (Greiner Bio-One, Kremsmünster, Austria, part no. 788096) with flat-bottomed 25 μL semi-conical wells. Triplicate batch experiments were used for all experiments. For all static experiments, a single bead was put into each well along with 20 μL of 7.5 M HNO_3, and contacted for 1 h. This solution was removed, and replaced with a 20 μL spike of ^{238}Pu in 7.5 M HNO_3 and allowed to remain in contact with the bead for times ranging from 1 min to 180 min. To minimize volume loss to evaporation parafilm was press-sealed over the top of each well. The solution was removed and counted by LSC. Process blanks indicated no Pu binding to the wells.

In the desorption study, Pu was sorbed onto the beads according to the process described above for 24 hr, these %M were compared to those obtained from the sorption experiments and were found to be within 1 σ. Pu loaded bead was then contacted with 20μL of 9 M HCl for 24 hrs, all of this solution was removed from each well and counted by LSC. Desorption was achieved by adding 20 μL 1.2 M HCl to each well containing a Pu loaded bead, contacting for times of 1 min to 1 week. The solution was removed from each well using a 200 μL pipettor, and was analyzed by LSC.

Dynamic Sorption and Desorption

Dynamic solution cycling experiments were conducted using 48,000 step digital syringe pumps (J-Kem Scientific, St. Louis, MO) equipped with 4 port distribution valves with either 0.25 mL or 0.5 mL syringes. For the dynamic experiments, one end of a 45.7 cm length of perfluoroalkoxy tubing (IDEX Health and Sciences) (inner diameter was dependent on the bead)

was connected to a port on the distribution valve. The other end was used with the resin bead trapped within a "reaction chamber"; created by crimping the tubing above and below the bead at 10 cm from the end of the tube. A diagram of the experimental apparatus can be seen in figure 1. All bead-in-tube assemblies were made identically. For the ~900 μm dia. SIR-1200 beads, an i.d. of 1000 μm was used; for the ~600 μm dia. SIR-1200 and Reillex-HPQ beads, an i.d. of 760 μm was used. The syringe pumps manipulated (aspirating and dispensing) 20 μL of the solution at a rate of 0.1 mL/min (adjusted to account for the two sizes of tubing).

For dynamic sorption experiments, 20 μL of 7.5 M HNO_3 was drawn up the tube and cycled across the bead for 5 min to rehydrate and convert the bead from the chloride form to nitrate form. This solution was removed before the introduction of the radionuclide. 20 μL of ^{238}Pu in 7.5 M HNO_3 was drawn into the tubing just below the bead, and cycled for 1 to 240 min and counted by LSC. No appreciable Pu sorption to the PFA tubing was found in the dynamic process blanks.

For the dynamic desorption 20 μL of the Pu solution in 7.5 M HNO_3 was cycled for 90 min. After the load, 20 μL of 9 M HCl added after the sorption process and cycled for 30 min. The solutions from each of the steps above were analyzed by LSC. Plutonium desorption was accomplished using 20 μL 1.2 M HCl by aspirating 1.2 M HCl for times of 1 to 120 min and counted by LSC.

The net activity from the LSC, for both static and dynamic experiments, were used to establish the percent of the analyte sorbed or desorbed from resin according to equation 5.

$$\%M = \frac{A_0 - A_f}{A_0} x100 \qquad 5$$

Where A_0 is the initial activity, A_f is the final activity after contact with the resin, and $\%M$ is the percent metal sorbed or eluted. No efforts were made to account for the small portion of Pu whose oxidation state changed. The $\%M$ reported for the desorption process reflect the percent of the ^{238}Pu removed from the bead after the sorption process and 9 M HCl contact step, and corrects for any desorption during the 9 M HCl rinse step. All reported %M values are the results of triplicate measurements and are shown in figures with 1 σ uncertainty. All linear fits are the result of fitting the initial rates up to 85% of the metal either sorbed or desorbed.

Results and Discussion

Sorption of ^{238}Pu

The uptake of ^{238}Pu as a function of time on single SIR-1200 and Reillex-HPQ beads are shown in Figures 2 A and B, respectively. Each plot compares the dynamic bead-in-a-tube method with static solution conditions. In all cases, the dynamic conditions were faster. Comparing the two graphs, ~900 μm SIR-1200 beads sorption rates are greater than ~600 μm Reillex-HPQ beads (made particularly apparent with the different magnitudes of the x-axes).

Figure 2 Here

Each plot in figure 2 A and B shows an inset plotting the –ln[X] as a function of time for each bead, with the rate constants determined by linear regression for data up to 85% Pu sorption.

Looking at the inset plots in figure 2, the rates of sorption were calculated using equation 1, resulting in rates of 1.6×10^{-4} s^{-1} (χ^2=0.013), and 7.6×10^{-4} s^{-1} (χ^2=0.030) for static and dynamic cycling conditions respectively, a 4.7 fold improvement. Comparison of literature is made difficult due to the limited study of single bead kinetic studies. Acoustic streaming provides the most directly comparable results, providing similar improvements in the rates to those found in this study. [5] Another comparison can be made to an advanced material, a superparamagnetic bi-functional composite bead, where equilibrium was established in 80 mins, a time lower than the times projected for the dynamic cycling conditions [7].

The diffusion layer thickness was calculated according to equation 3, using a value of 1.791×10^{-10} m^2/s for the diffusion coefficient, the volumes of the beads, and the observed rate constants above. Values of 141 μm and 30 μm for static and dynamic cycling respectively were calculated for the SIR-1200 experiments. These values fall within reason of literature values [8,22]. A similar decrease was seen when using acoustic streaming changing the diffusion layer thickness from 153 μm to 32 μm for a similar bead (AG 1x4, though smaller in diameter) [8].

The sorption on the Reillex-HPQ, according to figure 2 B, was significantly slower than the SIR-1200 bead. Dynamic cycling dramatically improved the rate of the sorption on Reillex-HPQ resulting in complete sorption in 2 hr. Examining the inset in figure 2B it shows rate constants of 3.2×10^{-5} s^{-1} (χ^2=0.011) and 5.1×10^{-4} s^{-1} (χ^2=0.0069) for static and dynamic cycling conditions, a 16 fold improvement. The diffusion layer thickness was calculated, decreasing from 335 μm to 21 μm. A value of 335 μm for the diffusion layer thickness is outside the expected values of 10-100 μm, it is possible that this is caused by the increased surface area of a macroporous bead [12-14].

Table 1 provides a summary of the observed ^{238}Pu sorption rate constants, the calculated values of the diffusion layer thickness, a comparison of the static and dynamic cycling conditions, and the linear regression fit parameters i.e. the number of points used in the fit and the resulting χ_2, and R^2.

A portion of the increase in the rate of the of the SIR-1200 bead sorption can be attributed to the larger size, a ~900 μm sphere has a surface area approximately 2.25x that of a ~600 μm sphere. A qualitative comparison of the sorption rates of similarly sized (~600 μm) Reillex-HPQ and SIR-1200 beads were made. The rate constants were found to be 5.1×10^{-4} s^{-1} and 4.7×10^{-4} s^{-1} for Reillex-HPQ and SIR-1200 respectively. The reported rate constant for the SIR-1200 is the result of singlet points and should be considered as is merely qualitative. The sorption rate similarities of the two bead types are supported well in the literature [10-13,15].

Desorption of ^{238}Pu

In an anion exchange separation to purify Pu, a load and wash step with 7.5 M nitric acid is conventionally followed by an elution step with 9 M HCl to convert the system to chloride form and to elute Th [28,29]. These steps were maintained in this work under both dynamic and static conditions, though Th was not investigated. Under dynamic conditions, 3.4(6)% and 4(1)% of the sorbed Pu was desorbed from the SIR-1200 and Reillex-HPQ beads respectively after 30-minute contacts. The quantity of Pu desorbed in 9 M HCl was 3(2)% in 24 hr for static conditions for both the SIR-1200 and Reillex-HPQ.

The desorption of ^{238}Pu with 1.2 M HCl as a function of time on single SIR-1200 and Reillex-HPQ beads are shown in figure 3 A and B respectively. The low acid concentration desorption is well known in the literature [8,11]. Dynamic was found to be a significant improvement over the static conditions. Comparing the two plots, the smaller Reillex-HPQ beads (~600 μm) desorb ^{238}Pu much faster than larger SIR-1200 beads (~900 μm). Similarly to figure 2, figure 3 A and B shows an inset plotting the –ln[X] as a function of time, determining the rate constants by linear regression for data up to 85% Pu desorption. Desorption kinetic studies are limited to column based examinations making direct comparisons difficult, though relative desorption kinetics have been discussed between strong base similar to SIR-1200, and Reillex-HPQ [12-14,29].

Figure 3 Here

It can be seen that complete Pu desorption from the SIR-1200 bead, as shown in figure 3A, occurs in about an hour using dynamic solution cycling conditions. Mirroring the results seen in the Pu sorption, complete Pu desorption was completed after 6 hours of static diffusion conditions, correlating to a roughly 5 fold increase in the desorption rates. Comparisons to literature are made difficult as there is no investigation of the desorption kinetics on single beads. Within the inset in figure 3A, rates of desorption were determined, producing rates of 1.4×10^{-4} s^{-1} (χ^2=0.0045), and 7.4×10^{-4} s^{-1} (χ^2= 6.0×10^{-5}) for static and dynamic cycling conditions respectively. Dynamic cycling conditions correspond directly to an increase of 5.3 fold.

Likewise, Figure 3B shows the desorption of Pu as a function of time on the Reillex-HPQ bead, the rate of desorption is significantly faster than seen with SIR-1200. This rapid Pu desorption rate is the hallmark of the Reillex-HPQ bead as seen by Marsh et al [12-14]. Complete desorption under static conditions was found to occur in ~2 hours. Under dynamic conditions complete Pu desorption occurred in ~ 30 mins. The inset of figure 3B was used to determine rate constants of 3.7×10^{-4} s^{-1} (χ^2=0.046) and 1.0×10^{-3} s^{-1} (χ^2=0.0063) for static and dynamic cycling conditions respectively, an improvement of 2.8 fold. Table 1 summarizes the ^{238}Pu sorption rate constants, a comparison of the static and dynamic cycling conditions, and the linear regression fit parameters i.e. number of points used in the fit and the resulting R^2.

Table 1 Here

Conclusion

The bead-in-a-tube method has shown its utility as a method to improve the sorption and desorption rates of Pu single bead micro-chemical purifications on commercially available single anion exchange beads. These improvements could be utilized to greatly reduce the processing time for ultralow level Pu samples destined for TIMS analysis. Currently, this method is being expanded to include Th and is being implemented as a source bead loading method and full separation scheme. Modifications to the bead-in-a-tube method would allow for adoption into other fields, but the method would conceivably be well suited for any number of micro-chemical processes including the preparation of radiochemical tracer standards [30].

Acknowledgments

The authors would like to thank Dr. Brienne Seiner for her assistance. This work was conducted in coordination with the National Nuclear Security Administration Office of Defense Nuclear Nonproliferation R&D's MSAP (Micro-Scale Automation Platform) project. Work was

performed at Pacific Northwest National Laboratory, which is operated for the Department of Energy by Battelle Memorial Institute under Contract DE-AC05-76RLO1830.

References

1. J.W. Grate, M.J. O'Hara, A.F. Faraila, M. Douglas, M.M. Haney, S.L. Peterson, T.C. Maiti, C.L. Aardahl, Extraction Chromatographic Methods in the Sample Preparation Sequence for Thermal Ionization Mass Spectrometric Analysis of Plutonium Isotopes, Anal. Chem. 83 (2011) 9086-9091. DOI:10.1021/ac202150v
2. J. Qiao, X. Hou, M. Miró, P. Roos, Determination of plutonium isotopes in waters and environmental solids: A review. Anal. Chim. Acta. 652 (2009) 66-84. DOI:10.1016/j.aca.2009.03.010
3. J. Zheng, K. Tagami, S. Uchida. Release of Pu isotopes into the environment from the Fukushima Daiichi Nuclear Power Plant Accident: What is known and what needs to be known. Environ. Sci. Tech. 47 (2018) 9584-9595.
4. C.R. Armstrong, P.R. Nuessle, H.A. Grant, G. Hall, J.E. Halverson, J.R. Cadieux. Plutonium Isotopes in Terrestrial Environment at the Savannah River Site, USA: A Long-Term Study. Environ. Sci. Tech. 49 (2015) 1286-1293. DOI: 10.1021/es504147d
5. M. Streat, Kinetics of Slow Diffusing Species in Ion Exchangers. React. Polym. 2 (1984) 79-91. DOI: 10.1016/0167-6989(84)90011-4.
6. M. Kiode, D.S. Lee, M.O. Stellard, Separation of trace metals from seawater using a single anion exchange bead. Anal. Chem. 56 (1984) 1956-1959. DOI: 10.1021/ac00275a04
7. R.L. Walker, R.E. Eby, C.A. Pritchard, J.A. Carter, Simultaneous plutonium and uranium isotopic analysis from a single bead: a simplified technique for assaying spent reactor fuel. Anal. Let. 7 (1974) 8-9. DOI: 10.1080/00032717408058789
8. W.F. Paxton, M.J. O'Hara, S.M. Peper, S.L. Petersen, J.W. Grate, Accelerated Analyte Uptake on Single Beads in Microliter Batch Separations Using Acoustic Streaming: Plutonium Uptake by Anion Exchange
9. Yao, C.; Chen, T. A new simplified method for estimating film mass transfer and surface diffusion coefficients from batch adsorption kinetic data. Chem. Eng. J. 265 (2015) 93-99.
10. Douven, S.; Paez, C.A.; Gommes, C.J. The range of validity of sorption kinetic models. J. Coll. Int. Sci. 448 (2015)437-450.
11. S.F. Marsh, G.D. Jarvinen, R.A. Bartsch, J. Nam, M.E. Barr, New bifunctional anion-exchange resins for nuclear waste treatment. J. Radioanal. Nucl. Chem. 235 (1998) 37-40. DOI:10.1007/BF02385934
12. J.M. Mannion, C.R. Shick Jr., G.A. Fugate, B. A. Powell, S.M. Husson. Anion-Exchange Fibers for Improved Sample Loading in Ultra-trace Analysis of Pu by Thermal Ionization Mass Spectrometry. Anal. Chem. 89 (2017) 8638-8642. DOI: 10.1021/acs.analchem.7b01455
13. J.M. Mannion, C.R. Shick Jr., G.A. Fugate, B.A. Powell, S.M. Husson. Anion exchange polymer filament coating for ultratrace isotopic analysis of plutonium by thermal ionization mass spectrometry. Talanta 189 (2018) 502-508.
14. R.U. Shah, S. Chappa, S.J. Kumar, A.M. Mhatre, S. Sahoo, R.M. Rao, P.G. Jaison, A.K. Pandy. Supported liquid membrane based loading technique for thermal ionization mass spectrometry: an application to isotopic composition and concentration determination. J. Radioanal. Nucl. Chem. 317 (2018) 1367-1376.
15. T. Kanazaki, S. Hirawa, M. Harada, T. Okada, Coupled Acoustic-Gravity Field for Dynamic Evaluation of Ion Exchange with a Single Resin Bead. Anal. Chem. 82 (2010) 4472-4478. DOI:10.1021/ac100275p
16. J.L. Ryan, Chemistry of Plutonium in Anion Exchange Applications. Proceedings of the US-UK Technical Exchange Meeting, Oak Ridge National Laboratory, Oak Ridge, TN, April 25-27, 1960, 2-20.
17. S.F. Marsh, Evaluation of a New, Macroporous Polyvinylpyridine Resin for Processing Plutonium Using Nitrate Anion Exchange*;* LA-11490; Los Alamos National Laboratory: Los Alamos, NM, 1989.
18. S. Paul, A.K. Pandey, R. V. Shah, D. Alamelu, S.K. Aggarwal, Superparamagnetic bi-functional composite bead for the thermal ionization mass spectrometry of plutonium (IV) ions. RSC Adv. 6 (2016) 3326-3334. DOI: 10.1039/c5ra18419c
19. S.F. Marsh, Improved Recovery and Purification of Plutonium at Los Alamos Using Macroporous Anion Exchange Resin*;* LA-10906; Los Alamos National Laboratory; Los Alamos, NM, 1987.
20. S.F. Marsh, K.D. Veirs, G.D. Jarvinen, M.E. Barr, E.W. Moody, Molecularly Engineered Resins for Plutonium Recovery. Los Alamos Sci. 26 (2000) 454-463.

21. G. Calleri, A. Geoffroy, F. Franssen, J. Demonie, Study of the Kinetics of Loading Pu(IV) Elution on Permutit SK Resin from 7.2 M Nitric Acid; NP-12345; ORNL: Oak Ridge, TN, 1961.

22. F. Helfferich, Ion Exchange, Dover Publications: Mineola, NY, 1995: Chapter 6, pp. 624.

23. D.G. Peters, W.D. Shults, Chronopotentiometry of Plutonium in Mineral Acid Media. J. Electroanal. Chem. 8 (1964) 200-229. DOI:10.1016/0022-0728(64)80115-7

24. V. Friehmelt, A. He, Z. Yang, G. Marx, The Measurement of Pu(VI) in Nitric Acid with the Aid of The Analytical Ultracentrifuge. Inorg. Chim. Acta. 109 (1985) L1-L2. DOI:10.1016/S0020-1693(00)86314-8

25. V. Friehmelt, A. He, Z. Yang, G. Marx, The Measurement of Pu(III) in Hydrochloric Acid with the Use of an Analytical Ultracentrifuge. Inorg. Chim. Acta. 109 (1985) L25-L26. DOI:10.1016/S0020-1693(00)81761-2

26. L.R. Morss, N.M. Edelstein, J. Fuger, Chapter 7 Plutonium. In The Chemistry of the Actinide and Transactinide Elements. Springer, Dodrecht, The Netherlands, 2008, Vol. 3, pp. 813-1264.

27. P.K. Mohapatra, L.B. Kumbhare, P.B. Ruikar, V.K. Manchanda, Ion-Exchange Separation of Pu from Macro Concentration of Th in HNO_3 Medium. Solv. Extr. Ion Exch. 22 (2004) 267-284. DOI:10.1081/SEI-120030462

28. E.K. Hulet, R.G. Gutmacher, M.S. Coops, Group Separation of the actinides from the lanthanides by anion exchange. J. Inorg. Nucl. Chem. 17 (1961) 350-360. DOI:10.1016/0022-1902(61)80161-9

29. G. Calleri, A. Geoffroy, F. Franssen, J. Demonie, Study of the Kinetics of Pu(IV) Elution from Permutit SK Resin, 40-70 mesh, at 60^{o}C by 0.6 M Nitric Acid; NP-12244; ORNL: Oak Ridge, TN, 1961.

.S. Snow, S.S. Morrison, S.B. Clark, J.E. Olson, M.G. Watrous, ^{237}Np analytical method using ^{239}Np tracers and application to a contaminated nuclear disposal facility. J. Environ. Radioact. 172 (2017) 89-95. DOI:10.1016/j.jenvrad.2017.02.018

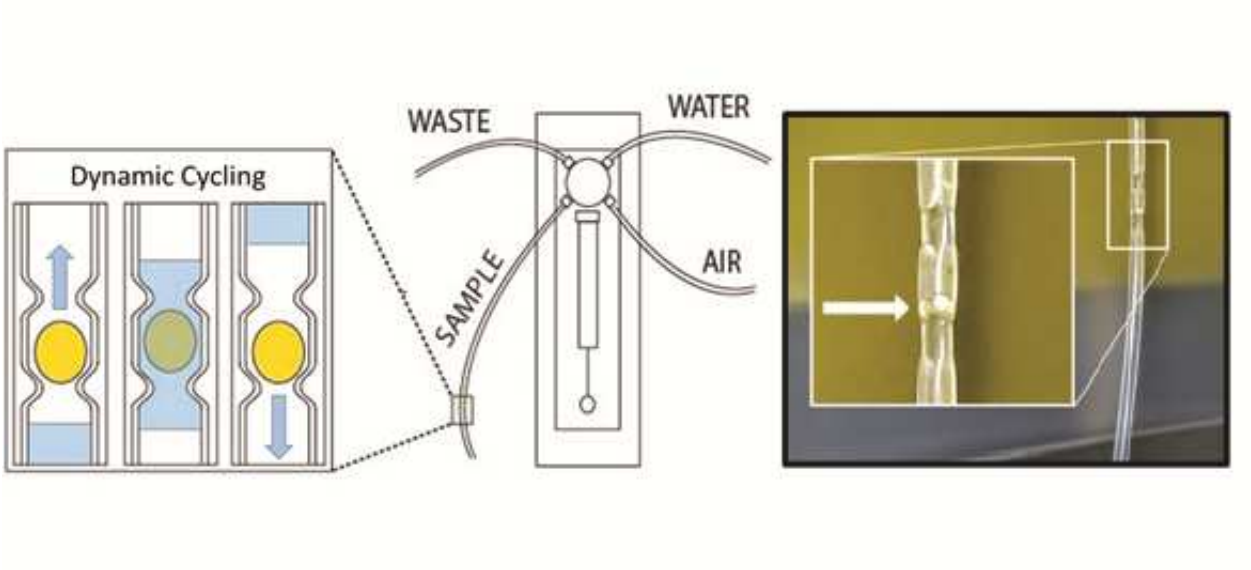

Figure 1. Left: Diagram of the bead-in-a-tube approach and apparatus for dynamic cycling of the solution over the surface of a single trapped anion exchange bead in "reaction chamber" created between crimps in the tubing. Right: Images of the reaction chamber with a 900 μm SIR-1200 trapped in 1 mm ID tubing.

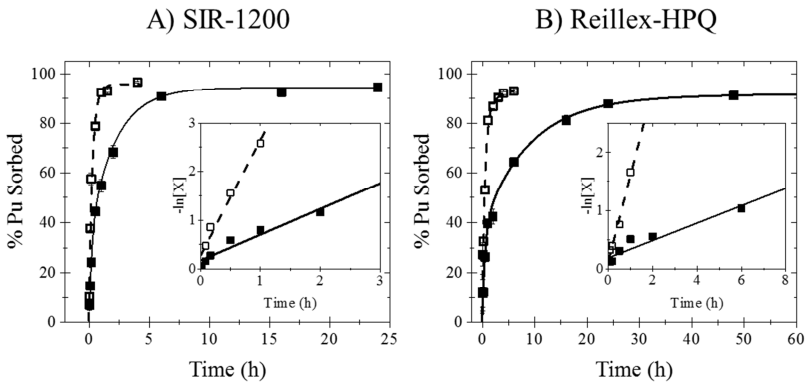

Figure 2. A) Percentage of ^{238}Pu sorbed to ~900 μm SIR-1200 and **B)** ~600 μm Reillex-HPQ as a function of time using static (■) or dynamic solution cycling conditions (□) at 0.1 mL/min. Dashed (static) or dotted (dynamic) lines are the fit from equation 1. The inset is the linear regression using equation 1 for both static (■) and dynamic (□) solution conditions.

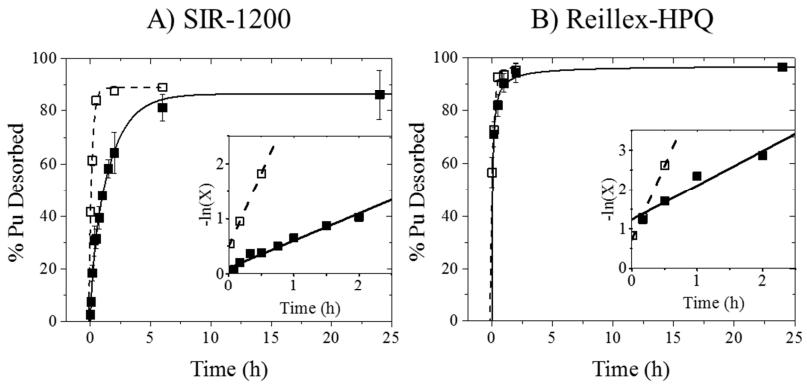

Figure 3. A) Percentage of ^{238}Pu desorbed to ~900 μm SIR-1200 and **B)** Percentage of ^{238}Pu desorbed from ~600 μm Reillex-HPQ as a function of time using static (■) or dynamic solution cycling conditions (□) at 0.1 mL/min. Dashed (static) or dotted (dynamic) lines are the fit from equation 1. The inset is the linear regression using equation 1 for both static (■) and dynamic (□) solution conditions, fitting the values < 85% Pu desorption. Exponential fit for static conditions on the Reillex-HPQ bead made use a point that is not included in the plot, this point was excluded to bring focus to the lower time points. The value for the 24 hour static contact with ~600 μm Reillex-HPQ was 96.5(5)%.

Table 1. Observed rate constants of static and dynamic cycling conditions for Pu sorption and desorption on both SIR-1200 and Reillex-HPQ beads. Diffusion layer thickness included for the sorption process only. Rate constants calculated from linear regression of data in figures 2 and 3, with reported uncertainty determined by Origin 2017.

SORPTION							
Bead type	**Contact Conditions**	**Rate (s^{-1}) [c]**	**Times faster than static diffusion [d]**	**N [e]**	**R^2**	**χ^2**	**δ_{obs} (μm) [f]**
SIR-1200 [a]	Static	$1.6(2)\times10^{-4}$	1	6	0.95	0.013	141
	Dynamic	$7.6(5)\times10^{-4}$	4.7	5	0.99	0.030	30
Reillex-HPQ [b]	Static	$3.2(3)\times10^{-5}$	1	8	0.95	0.011	335
	Dynamic	$5.1(4)\times10^{-4}$	15.9	5	0.98	0.0069	21
DESORPTION							
Bead type	**Contact Conditions**	**Rate (s^{-1}) [c]**	**Times faster than static diffusion [d]**	**N [e]**	**R^2**	**χ^2**	
SIR-1200 [a]	Static	$1.4(1)\times10^{-4}$	1	9	0.97	0.0045	
	Dynamic	$7.4(1)\times10^{-4}$	5.3	3	0.99	6.0×10^{-5}	
Reillex-HPQ [b]	Static	$3.7(1)\times10^{-4}$	1	4	0.99	0.046	
	Dynamic	$1.0(1)\times10^{-3}$	2.8	3	0.99	0.0063	

a. ~900 μm SIR-1200 beads were used

b. ~600 μm Reillex-HPQ beads were used

c. Parentheses enclose the uncertainty in the last reported digit

d. Average over the time intervals with < 85% sorption or desorption

e. Number of points used in the linear regression and are the average of triplicate measurements

f. Calculated diffusion layer thickness using the $\delta=3\tilde{V}D/r_oVk_{obs}$.